SCIENCE CHINA
Technological Sciences

Special Topic: Current Progress in Solid Mechanics and Physical Mechanics
•Article•

May 2019 Vol.62 No.5: 787–798
https://doi.org/10.1007/s11431-018-9427-9

A frequency domain reliability analysis method for electromagnetic problems based on univariate dimension reduction method

PING MengHao[1], HAN Xu[1*], JIANG Chao[1], ZHONG JianFeng[2], XIAO XiaoYa[1], HUANG ZhiLiang[1] & WANG ZhongHua[1]

[1] *State Key Laboratory of Advanced Design and Manufacturing for Vehicle Body, College of Mechanical and Vehicle Engineering, Hunan University, Changsha 410082, China;*
[2] *Nanjing Research Institute of Electronics Technology, Nanjing 210039, China*

Received October 10, 2018; accepted January 2, 2019; published online March 29, 2019

In this paper, a class of electromagnetic field frequency domain reliability problem is first defined. The frequency domain reliability refers to the probability that an electromagnetic performance indicator can meet the intended requirements within a specific frequency band, considering the uncertainty of structural parameters and frequency-variant electromagnetic parameters. And then a frequency domain reliability analysis method based on univariate dimension reduction method is proposed, which provides an effective calculation tool for electromagnetic frequency domain reliability. In electromagnetic problems, performance indicators usually vary with frequency. The method firstly discretizes the frequency-variant performance indicator function into a series of frequency points' functions, and then transforms the frequency domain reliability problem into a series system reliability problem of discrete frequency points' functions. Secondly, the univariate dimension reduction method is introduced to solve the probability distribution functions and correlation coefficients of discrete frequency points' functions in the system. Finally, according to the above calculation results, the series system reliability can be solved to obtain the frequency domain reliability, and the cumulative distribution function of the performance indicator can also be obtained. In this study, Monte Carlo simulation is adopted to demonstrate the validity of the frequency domain reliability analysis method. Three examples are investigated to demonstrate the accuracy and efficiency of the proposed method.

electromagnetic field, frequency domain reliability, system reliability, random process discretization, univariate dimension reduction method

Citation: Ping M H, Han X, Jiang C, et al. A frequency domain reliability analysis method for electromagnetic problems based on univariate dimension reduction method. Sci China Tech Sci, 2019, 62: 787–798, https://doi.org/10.1007/s11431-018-9427-9

1 Introduction

In electromagnetic problems, the antenna system is a complex system integrating electromagnetic transmission and electromagnetic radiation, and it is an important application of electromagnetic theory. Its frequency domain performance indicators are the main goal of design and optimization. At present, there have been a lot of researches on the design and optimization for the frequency-variant performance indicators of broadband antenna and array antenna.

In terms of broadband antenna design, Jung [1] designed an L-type microstrip monopole antenna with a reflection coefficient less than –10 dB in the frequency band of 3.05–10.9 GHz, which reduces the reflection loss of the antenna and improves radiation pattern characteristics. Abbas-Azimi et al. [2] proposed a design method for broadband horn antenna, so that its beamwidth and maximum gain in the given frequency band meet the requirements. Yang et al. [3] proposed a novel circularly polarized microstrip antenna that effectively increases the axial ratio bandwidth and gain

*Corresponding author (email: hanxu@hnu.edu.cn)

compared to conventional microstrip antennas while reducing reverse radiation. Klymyshyn et al. [4] studied the impact of TML parameters on the antenna performance when low-loss and lossy substrates are used and proposed two different TML-DRA structures, increasing the impedance bandwidth of the antenna and improving the radiation efficiency. As for the optimization of antenna frequency domain performances, Choo et al. [5] used genetic algorithm to optimize the patch shape of broadband and dual-band microstrip antennas to improve their impedance bandwidth. Mohamadi Monavar et al. [6] used the invasive weed optimization (IWO) algorithm to design the geometric parameters of the microstrip patch antenna, and reduced the return loss in the frequency band while maintaining the gain and radiation pattern. Abbas-Azimi et al. [7] found the main parameters affecting the gain of the main lobe by analyzing the sensitivity of the traditional broadband double-ridge horn antenna structure parameters, and it was optimized using the quasi-Newton method to obtain a better radiation pattern in high frequency and VSWR in the frequency band. In the design and optimization of the array antenna frequency domain performances, Pourahmadazar et al. [8] proposed a broadband circularly-polarized monopole antenna, and enhanced the frequency domain performance on impedance matching and circular polarization by adjusting the location of the monopole microstrip-feed. El-makadema et al. [9] used genetic algorithm and pattern search technology to optimize the array geometry, achieving the enhancement of its performances such as directivity, sidelobe characteristics and beamwidth in frequency band. Wang et al. [10] focused on the maximization of the system effective multiplexing gain in the frequency band, by optimizing the individual antenna positions in the transmit/receive non-uniform linear antenna arrays.

In the frequency domain performance study of components, Okabe et al. [11] designed a new type of hybrid ring, and optimized its characteristic impedance and transmission loss in the high frequency range, while reducing the structure size. Kim et al. [12] proposed a simple parametric modeling method for frequency-variant transmission lines. The effects of frequency-dependent parameters such as dielectric constant, propagation constant and characteristic impedance on the reflection coefficient were analyzed in a broad frequency range from 40 MHz to 50 GHz, and experimental verification was carried out. You et al. [13] proposed a method to find the optimum source and load impedances that make the device perform well in efficiency and flat gain within the required bandwidth.

The above electromagnetic problems are only for the effect of deterministic input parameters on the performance indicators in the design frequency band. While in practical problems, the uncertainty of structural parameters and frequency-variant electromagnetic parameters will affect the frequency-variant performance indicators (such as impedance, gain, reflection coefficient), so the performance indicators will be changed from determined value to uncertainty. Furthermore their uncertainty varies with frequency, causing their reliability to vary with frequency. Considering the probability that a performance indicator meets specific design requirement within a specific frequency band, it constitutes a frequency domain reliability problem. Aiming at those above problems, we propose a frequency domain reliability analysis method based on univariate dimension reduction method (FRDR), which provides an effective calculation tool for frequency domain reliability of electromagnetic problems. Based on the idea of random process discretization [14], we discretize the frequency domain into frequency points, thus producing a series of discrete frequency points' functions.

Then FRDR is employed to convert the frequency domain reliability problem into a series system reliability problem concerning discrete frequency points. To solve the reliability at each discrete frequency point, there are many traditional methods such as FORM [15–17], SORM [18,19], etc. However, when those above methods meeting engineering problems, we have to use the surrogate model, or directly calculate the derivative of the finite element function, and that may have a bad effect on the computing efficiency and accuracy. Furthermore, it will cause more computing efforts for solving the correlation coefficients of all the discrete frequency points' functions.

Therefore, this paper uses the univariate dimension reduction method (UDRM) [20–22] to solve the probability distribution functions (PDFs) of the discrete frequency points' functions in the system. Thus when solving the correlation coefficient matrix, we can reuse the calculation results of the functions which have been solved when calculating the PDFs. In this way, FRDR simplifies the analysis process, resulting in higher efficiency and much better practicability.

2 Frequency domain reliability problem

Performance indicators usually vary with frequency in electromagnetic problems. Considering the influence of uncertain parameters on it, the frequency domain reliability of the electromagnetic problems is defined as: considering the uncertainty of structural parameters and frequency-variant electromagnetic parameters, the probability that a performance indicator can meet the intended requirements within a specific frequency band. According to the definition of reliability, the failure probability $P(f_{\mathrm{L}},f_{\mathrm{U}})$ of an electromagnetic performance indicator in the frequency band $[f_{\mathrm{L}},f_{\mathrm{U}}]$ is [23]

$$P(f_{\mathrm{L}},f_{\mathrm{U}}) = P\{g(\mathbf{X}(f),\mathbf{Y},f) < 0, \forall f \in [f_{\mathrm{L}},f_{\mathrm{U}}]\}, \quad (1)$$

where f is frequency, $P\{\cdot\}$ represents probability calculation, $g(\cdot)$ is the performance indicator function, $\mathbf{X}(f)=$ $=[X_1(f),X_2(f),...,X_m(f)]$ is a m-dimensional random process vector, $\mathbf{Y}=(Y_1,Y_2,...,Y_n)$ is a n-dimensional random vector.

The reliability analysis method based on Monte Carlo simulation (MCS) is the most basic method for calculating the reliability problem, and can also be used in the frequency domain reliability analysis. First, MCS is used to sample random process vector $\mathbf{X}(f)$ and random vector $\mathbf{Y}$ to obtain N groups of samples $[\overline{\mathbf{X}}_i(f),\overline{\mathbf{Y}}_i], i=1,2,...,N$. Take these samples into $\mathbf{X}(f)$ and $\mathbf{Y}$ of the function $g(\mathbf{X}(f),\mathbf{Y},f)$, we can obtain N deterministic frequency functions $g(\overline{\mathbf{X}}_i(f),\overline{\mathbf{Y}}_i,f), i=1,2,...,N$. The function corresponding to the i-th group of samples is expressed as $g(\overline{\mathbf{X}}_i(f),\overline{\mathbf{Y}}_i,f)$. Then, find the minimum value in the design frequency band $[f_{\mathrm{L}},f_{\mathrm{U}}]$ of each deterministic frequency function. And if it is less than 0, the corresponding group of samples is considered to be failure. Finally, count the number of failed groups n_f, the failure probability equals the number of failed groups divided by the total number of groups, i.e. $P(f_{\mathrm{L}},f_{\mathrm{U}}) = n_f / N$.

3 Frequency domain reliability analysis method based on univariate dimensional reduction method

The above MCS requires a large number of function evaluations, which often causes excessive computational cost in engineering problems. In this paper, with reference to random process discretization and based on UDRM, we propose FRDR, which not only avoids the expensive computational cost of MCS, but also is an accurate calculation tool for frequency domain reliability analysis.

The flow chart of FRDR is shown in Figure 1. By discretizing the frequency domain function into discrete frequency points' functions, we first convert the frequency domain reliability problem into a series system reliability problem of the discrete functions. Then UDRM is employed to solve the PDFs of the discrete functions and the correlation coefficient matrix in the system. Finally, corresponding to the PDFs and the correlation coefficient matrix, frequency domain reliability can be obtained by calculating the system reliability and the cumulative distribution function (CDF) of the frequency domain function can also be obtained. In this way, after solving the PDFs, it is not necessary to call the function again to calculate the correlation coefficients, but to establish a corresponding method to directly obtain the correlation coefficient matrix by using the previous calculation results, thus improving the efficiency of the method. While for solving the CDF of the frequency domain function, we only need to repeatedly calculate the system reliability of different failure thresholds, without increasing the number of calls to the function.

3.1 Transformation and calculation of the system reliability

Discretizing the frequency domain function over $[f_{\mathrm{L}}, f_{\mathrm{U}}]$ in eq. (1) at p+1 frequency points, we can get a series system reliability problem with p+1 functions, which can be expressed as follows [17]:

$$P(f_{\mathrm{L}},f_{\mathrm{U}}) = 1 - P\left\{\bigcap_{i=0}^{p}\left[g_i\left(\mathbf{X}(f_i),\mathbf{Y},f_i\right) > 0, f_i = i\Delta f, \Delta f = \frac{f_{\mathrm{U}}-f_{\mathrm{L}}}{p}\right]\right\}, \quad (2)$$

where $g_i\left(\mathbf{X}(f_i),\mathbf{Y},f_i\right)$ is the function at the i-th frequency point f_i, $\mathbf{X}(f_i)=[X_1(f_i),X_2(f_i),...,X_m(f_i)]$ is the random vector of $\mathbf{X}(f)$ at f_i, the correlation coefficient matrix $\mathrm{COV}(\mathbf{X}(f_i))$ can be obtained by the cross-correlation function matrix of $\mathbf{X}(f)$.

Define $g_i\left(\mathbf{X}(f_i),\mathbf{Y}\right) = g\left(\mathbf{X}(f_i),\mathbf{Y},f_i\right), i=1,2,...,p$. Due to the correlation among the functions at discrete frequency points, the functions $g_i, i=1,2,...,p$, can be regarded as a set of correlated random variables, of which the marginal probability density function f_{g_i} and correlation coefficient matrix ρ can be solved by UDRM and maximum entropy method (MEM) [24]. According to the method of series system reliability analysis [25], the eq. (2) can be calculated by the follows:

$$\begin{aligned} P\left\{\bigcap_{i=0}^{p} g_i > 0\right\} &= \int_0^{+\infty}...\int_0^{+\infty} f_{g_0,...g_p}\,\mathrm{d}g_0...\mathrm{d}g_p \\ &= \Phi_{p+1}\left[\Phi^{-1}\left(F_{g_0}(0)\right),...,\Phi^{-1}\left(F_{g_i}(0)\right),...,\right. \\ &\quad \left.\Phi^{-1}\left(F_{g_p}(0)\right),\rho'\right], \end{aligned} \quad (3)$$

where $f_{g_0,...,g_p}$ is the joint probability density function of $g_0,...,g_p$, $\Phi_{p+1}(\cdot)$ is the $p+1$-dimensional standard gaussian distribution function, F_{g_i} is the marginal cumulative distribution function of g_i, $\boldsymbol{\rho}'$ is the new correlation coefficient matrix converted from $\boldsymbol{\rho}$ after Nataf transformation.

In system reliability problem, when two random variables are identically distributed and the correlation between them is close to 1, the two correlated variables can be regarded as one variable, which has little effect on the calculation ac-

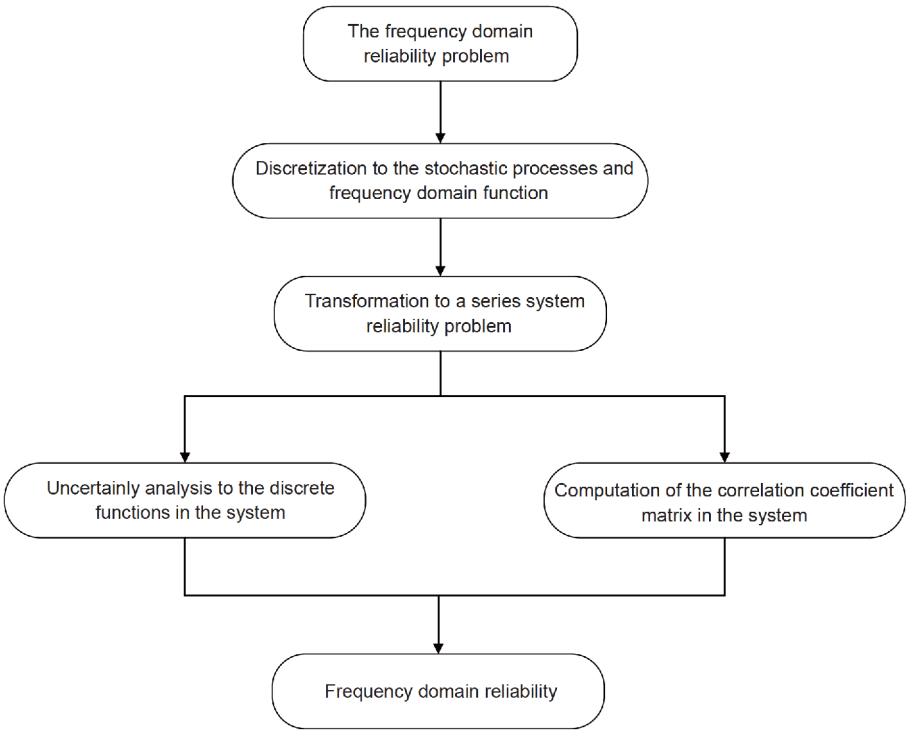

Figure 1 The flow chart of FRDR.

curacy. This characteristic can be used to define the convergence condition of the quantity of discrete frequency points. In eq. (3), the quantity of discrete frequency points is iterated until the correlation of arbitrarily adjacent two functions reaches a certain value $\overline{\rho}$ (less than 1), which is the convergence index set by us. For engineering problems, this convergence index will be used to balance the calculation efficiency and calculation accuracy.

It is worth noting that, there is a difference between the problem above and the conventional series system reliability problem, because all the components of the latter usually share the same input random variables, while the components of the former do not. For example, $g_i\left(\mathbf{X}(f_i),\mathbf{Y}\right)$ has an input random vector $\mathbf{X}(f_i)$ while $g_j\left(\mathbf{X}(f_j),\mathbf{Y}\right)(j\neq i)$ has another input random vector $\mathbf{X}(f_j)$ which is correlated to $\mathbf{X}(f_i)$. As a consequence of that, the calculation of ρ in this study is different from that in the conventional series system reliability problem. The following two subsections will detail the calculation of the above mentioned f_{g_i} and $\boldsymbol{\rho}$ separately.

3.2 Uncertainty analysis of the discrete frequency point's function

For simplicity, hereinafter all the random processes in $\mathbf{X}(f)$ are assumed to be mutually independent and so are the random variables in $\mathbf{Y}$. In the uncertainty analysis of the i-th frequency point's function $g_i\left(\mathbf{X}(f_i),\mathbf{Y}\right)$, UDRM is adopted to solve the first n-th statistical moments, from which the PDF f_{g_i} can be obtained by MEM. So we calculate the moments first. The k-th moment about zero of $g_i\left(\mathrm{X}(f_i),\mathbf{Y}\right)$ is expressed as

$$\mu_k=\mathrm{E}\left[{g_i}^k\left(\mathbf{X}(f_i),\mathbf{Y}\right)\right]=\iint_{\boldsymbol{\Omega}}{g_i}^k f_{X(f_i)}f_{\mathbf{Y}}\mathrm{d}\mathbf{X}(f_i)\mathrm{d}\mathbf{Y}, \tag{4}$$

in which E represents the expectation operator, Ω is the integral domain, $f_{X(f_i)}$ is the joint PDF of the random vector $\mathbf{X}(f_i)=[X_1(f_i),X_2(f_i),\ldots,X_m(f_i)]$, $f_{\mathbf{Y}}$ is the joint PDF of the random vector $\mathbf{Y}=[Y_1,Y_2,\ldots,Y_n]$.

There are $m+n$ variables in $g_i\left(\mathbf{X}(f_i),\mathbf{Y}\right)$, which may cause the integral in eq. (4) cannot be evaluated analytically. UDRM [20–22] involves an additive decomposition of a multi-dimensional response function into multiple one-dimensional functions, and approximate the response moments by the moments of one-dimensional functions. By UDRM, $g_i\left(\mathbf{X}(f_i),\mathbf{Y}\right)$ can be expressed as

$$\begin{aligned}g_i\left(\mathbf{X}(f_i),\mathbf{Y}\right)&=g_i(X_1(f_i),X_2(f_i),\ldots,X_m(f_i),Y_1,Y_2,\ldots,Y_n)\\&\approx-(m+n-1)g_{i,0}+\sum_{u=1}^{m}g_{i,X_u}+\sum_{v=1}^{n}g_{i,Y_v},\end{aligned} \tag{5}$$

in which $g_{i,0}$ represents $g_i\left(\boldsymbol{\mu}_{X(f_i)},\boldsymbol{\mu}_Y\right)$, g_{i,X_u} represents $g_i\left(\mu_{X_1(f_i)},...,\mu_{X_{u-1}(f_i)},X_u(f_i),\mu_{X_{u+1}(f_i)},...,\mu_{X_m(f_i)},\boldsymbol{\mu}_Y\right)$, g_{i,Y_v} represents $g_i\left(\boldsymbol{\mu}_{X(f_i)},\mu_{Y_1},...,\mu_{Y_{v-1}},Y_v,\mu_{Y_{v+1}},...,\mu_{Y_n}\right)$, $\boldsymbol{\mu}_{X(f_i)}$ is the mean of $\mathbf{X}(f_i)=[X_1(f_i),X_2(f_i),...,X_m(f_i)]$, $\boldsymbol{\mu}_Y$ is the mean of $\mathbf{Y}=[Y_1,Y_2,...,Y_n]$. Bring eq. (5) into eq. (4), the k-th moment about zero of $g_i\left(\mathbf{X}(f_i),\mathbf{Y}\right)$ can be approximated as

$$\begin{aligned}\mu_k &= \mathrm{E}\left[{g_i}^k\left(\mathbf{X}(f_i),\mathbf{Y}\right)\right]\\ &\approx \mathrm{E}\left[\left\{-(m+n-1)g_{i,0}+\sum_{u=1}^{m}\mathrm{g}_{i,X_u}+\sum_{v=1}^{n}\mathrm{g}_{i,Y_v}\right\}^k\right].\end{aligned}\tag{6}$$

Applying the binomial formula on the right-hand side of eq. (6) gives

$$\begin{aligned}\mu_k &\approx \sum_{l=0}^{k}\binom{k}{l}\mathrm{E}\left\{\sum_{u=1}^{m}\mathrm{g}_{i,X_u}+\sum_{v=1}^{n}\mathrm{g}_{i,Y_v}\right\}^l\left[-(m+n-1)g_{i,0}\right]^{k-l}\\ &= \sum_{l=0}^{k}\binom{k}{l}\left\{\sum_{q=0}^{l}\binom{l}{q}\mathrm{E}\left[\sum_{u=1}^{m}\mathrm{g}_{i,X_u}\right]^q\mathrm{E}\left[\sum_{v=1}^{n}\mathrm{g}_{i,Y_v}\right]^{l-q}\right\}^l\\ &\quad\times\left[-(m+n-1)g_{i,0}\right]^{k-l}.\end{aligned}\tag{7}$$

Define

$$S_u^{\,q}=\mathrm{E}\left[\left\{\sum_{j=1}^{u}\mathrm{g}_{i,X_j}\right\}^q\right],\tag{8}$$

$$R_v^{\,l-q}=\mathrm{E}\left[\left\{\sum_{j=1}^{v}\mathrm{g}_{i,Y_j}\right\}^{l-q}\right],\tag{9}$$

in which $u=1,\cdots,m$, $v=1,\cdots,n$, $q=1,\cdots,l$, $l=1,\cdots,k$. Using the recursive formula gives

$$\begin{aligned}&S_1^{\,q}=\mathrm{E}\left[(\mathrm{g}_{i,X_1})^q\right];\qquad q=1,\cdots,l,\\ &S_2^{\,q}=\sum_{p=0}^{q}\binom{q}{p}{S_1}^p\mathrm{E}\left[(\mathrm{g}_{i,X_2})^{q-p}\right];\ q=1,\cdots,l,\\ &\vdots\\ &S_u^{\,q}=\sum_{p=0}^{q}\binom{q}{p}{S_{u-1}}^p\mathrm{E}\left[(\mathrm{g}_{i,X_u})^{q-p}\right];\ q=1,\cdots,l,\\ &\vdots\\ &S_m^{\,q}=\sum_{p=0}^{q}\binom{q}{p}{S_{m-1}}^p\mathrm{E}\left[(\mathrm{g}_{i,X_m})^{q-p}\right];\ q=1,\cdots,l,\end{aligned}\tag{10}$$

$$\begin{aligned}&R_1^{\,l-q}=\mathrm{E}\left[(\mathrm{g}_{i,Y_1})^{l-q}\right];\qquad l-q=1,\cdots,l,\\ &R_2^{\,l-q}=\sum_{p=0}^{l-q}\binom{l-q}{p}{S_1}^p\mathrm{E}\left[(\mathrm{g}_{i,Y_2})^{l-q-p}\right];\ l-q=1,\cdots,l,\\ &\vdots\\ &R_v^{\,l-q}=\sum_{p=0}^{l-q}\binom{l-q}{p}{S_{v-1}}^p\mathrm{E}\left[(\mathrm{g}_{i,Y_v})^{l-q-p}\right];\ l-q=1,\cdots,l,\\ &\vdots\\ &R_n^{\,l-q}=\sum_{p=0}^{l-q}\binom{l-q}{p}{S_{n-1}}^p\mathrm{E}\left[(\mathrm{g}_{i,Y_n})^{l-q-p}\right];\ l-q=1,\cdots,l.\end{aligned}\tag{11}$$

Hence, eq. (7) becomes

$$\mu_k\approx\sum_{l=0}^{k}\binom{k}{l}\left[\sum_{q=0}^{l}\binom{l}{q}S_m^{\,q}R_n^{\,l-q}\right]\left[-(m+n-1)g_{i,0}\right]^{k-l}.\tag{12}$$

In eqs. (10) and (11), one needs to compute $\mathrm{E}\left[(\mathrm{g}_{i,X_u})^q\right]$ and $\mathrm{E}\left[(\mathrm{g}_{i,Y_v})^q\right]$, $q=1,\cdots,l$. According to the definition of expectation

$$\mathrm{E}\left[(\mathrm{g}_{i,X_u})^q\right]=\int_{-\infty}^{+\infty}(\mathrm{g}_{i,X_u})^q f_{X_u(f_i)}(x_u)\mathrm{d}x_u,\tag{13}$$

$$\mathrm{E}\left[(\mathrm{g}_{i,Y_v})^q\right]=\int_{-\infty}^{+\infty}(\mathrm{g}_{i,Y_v})^q f_{Y_v}(y_v)\mathrm{d}y_v,\tag{14}$$

where $f_{X_u(f_i)}$ is the PDF of $X_u(f_i)$, f_{Y_v} is the PDF of Y_v. The numerical integration method is used to solve the above series of univariate integrals, and then bring the result into eq. (12) to obtain the k-th moment about zero of $g_i\left(\mathbf{X}(f_i),\mathbf{Y}\right)$.

MEM [26] can be used for estimating the PDF of a random variable based on its statistical moments. The principle of maximum entropy can be described as follows: under given statistical moments, there exist a lot of possible probability distributions, one of which can maximize the information entropy is the least biased, and that is the maximum entropy probability distribution. Now we take the statistical moments of $g_i\left(\mathbf{X}(f_i),\mathbf{Y}\right)$ as constraints, and use MEM to find the PDF of $g_i\left(\mathbf{X}(f_i),\mathbf{Y}\right)$.

Define $f_{\mathrm{g}_i}(g_i)$ as the PDF of g_i, then its information entropy H is

$$H=-\int_{\Omega}f_{\mathrm{g}_i}(g_i)\ln f_{\mathrm{g}_i}(g_i)\mathrm{d}g_i,\tag{15}$$

in which Ω is the integral domain.

Take the first k-th moments about zero $\mu_r, r=0,1,...,k$, as constraints, maximizing the eq. (15) gives

$$\begin{aligned}&\max\ H\\ &\text{s.t.}\ \ \mu_r=\mathrm{E}\left({g_i}^r\right)=\int_{\Omega}{g_i}^r f_{g_i}(g_i)\mathrm{d}g_i,\quad r=0,1,...,k.\end{aligned}\tag{16}$$

Based on the Lagrange multiplier method [27] and by introducing modified function, the maximum entropy probability density function is obtained as

$$f_{g_i}(g_i) = \exp\left(\sum_{r=0}^{k} a_r {g_i}^r\right), \tag{17}$$

in which a_r is the undefined parameter. Taking eq. (17) into eq. (16), there yields a set of nonlinear equations

$$\mu_r = \int_\Omega {g_i}^r \exp\left(\sum_{r=0}^{k} a_r {g_i}^r\right) \mathrm{d}g_i, \quad r = 0, 1, ..., k. \tag{18}$$

Usually, we use the first four-order statistical moments as constraints. According to the statistical moments, the coefficients a_r, $r = 0, 1, ..., k$, can be obtained by solving eq. (18), then bringing them into eq. (17) can obtain the maximum entropy probability density function f_{g_i} of g_i.

3.3 Calculation of the correlation coefficient matrix

In the subsection, we will give an approach to calculate the correlation coefficient matrix ρ for solving eq. (3). $\rho_{i,j}$ is an component of ρ which represents the correlation coefficient between g_i and g_j, and it can be expressed as

$$\rho_{i,j} = \frac{\mathrm{E}(g_i g_j) - \mu_{g_i}\mu_{g_j}}{\sigma_{g_i}\sigma_{g_j}}, \tag{19}$$

in which μ_{g_i}, μ_{g_j} are the means of g_i, g_j respectively, $\sigma_{g_i}, \sigma_{g_j}$ are the standard deviations of g_i, g_j respectively, and they all can be solved by the uncertainty analysis in Sect. 3.2. $\mathrm{E}(g_i g_j)$ can be calculated by

$$\begin{aligned}\mathrm{E}(g_i g_j) &= \iint g_i g_j f_{g_i, g_j} \mathrm{d}g_i \mathrm{d}g_j \\ &= \iiint g_i\left(X(f_i), Y\right) g_j\left(X\left(f_j\right), Y\right) \\ &\quad \times f_{X(f_i), X\left(f_j\right)} f_{\mathbf{Y}} \mathrm{d}X(f_i) \mathrm{d}X\left(f_j\right) \mathrm{d}\mathbf{Y},\end{aligned} \tag{20}$$

where $X(f_i), X\left(f_j\right)$ are the random vector of $\mathbf{X}(f)$ at i-th and j-th frequency point respectively, $f_{X(f_i), X\left(f_j\right)}$ is the joint PDF. Because of the independence of the components in $X(f)$, we can obtain $f_{X(f_i), X\left(f_j\right)} = f_{X_1(f_i), X_1\left(f_j\right)} f_{X_2(f_i), X_2\left(f_j\right)} \cdots f_{X_m(f_i), X_m\left(f_j\right)}$, any one of them $f_{X_k(f_i), X_k\left(f_j\right)}, k = 1, 2, ..., m$, can be fitted by gaussian copula function [28]:

$$\begin{aligned}&f_{X_k(f_i), X_k\left(f_j\right)} \\ &= f_{X_k(f_i)} f_{X_k\left(f_j\right)} \left|\boldsymbol{\rho}_k\right|^{-1/2} \\ &\exp\left\{\left[\Phi^{-1}\left(f_{X_k(f_i)}\right), \Phi^{-1}\left(f_{X_k\left(f_j\right)}\right)\right]\left[\boldsymbol{\rho}_k^{-1} - \mathbf{I}\right]\right. \\ &\left.\times\left[\Phi^{-1}\left(f_{X_k(f_i)}\right); \Phi^{-1}\left(f_{X_k\left(f_j\right)}\right)\right]\right\},\end{aligned} \tag{21}$$

where $f_{X_k(f_i)}, f_{X_k\left(f_j\right)}$ are the marginal PDF of $X_k(f_i)$ and $X_k\left(f_j\right)$ respectively, $\boldsymbol{\rho}_k$ is the correlation coefficient matrix of $X_k(f_i)$ and $X_k\left(f_j\right)$, $\mathbf{I}$ represents unit matrix. Expand g_i and g_j respectively using UDRM described above

$$g_i(X_i, Y, f_i) \approx -(m+n-1)g_{i,0} + \sum_{u=1}^{m} \mathrm{g}_{i,X_u} + \sum_{v=1}^{n} \mathrm{g}_{i,Y_v}, \tag{22}$$

$$g_j\left(X_j, Y, f_j\right) \approx -(m+n-1)g_{j,0} + \sum_{u=1}^{m} \mathrm{g}_{j,X_u} + \sum_{v=1}^{n} \mathrm{g}_{j,Y_v}. \tag{23}$$

Take eq. (22) and (23) into eq. (20)

$$\begin{aligned}&\mathrm{E}(g_i g_j) = \iint g_i g_j f_{g_i, g_j} \mathrm{d}g_i \mathrm{d}g_j \\ &= (m+n-1)^2 g_{i,0} g_{j,0} - (m+n-1)g_{i,0} \\ &\times\left(\sum_{u=1}^{m} \int \mathrm{g}_{j,X_u} f_{X_u\left(f_j\right)}(x_u)\mathrm{d}x_u + \sum_{v=1}^{n} \int \mathrm{g}_{j,Y_v} f_{Y_v}(y_v)\mathrm{d}y_v\right) \\ &-(m+n-1)g_{j,0} \\ &\times\left(\sum_{u=1}^{m} \int \mathrm{g}_{i,X_u} f_{X_u(f_i)}(x_u)\mathrm{d}x_u + \sum_{v=1}^{n} \int \mathrm{g}_{i,Y_v} f_{Y_v}(y_v)\mathrm{d}y_v\right) \\ &+ \sum_{u_1=1}^{m}\sum_{u_2=1}^{m} \iint \mathrm{g}_{i,X_{u_1}} \mathrm{g}_{j,X_{u_2}} f_{X_{u_1}(f_i), X_{u_2}\left(f_j\right)}(x_{u_1}, x_{u_2})\mathrm{d}x_{u_1}\mathrm{d}x_{u_2} \\ &+ \sum_{u=1}^{m}\sum_{v=1}^{n} \iint \mathrm{g}_{i,X_u} \mathrm{g}_{j,Y_v} f_{X_u(f_i)}(x_u) f_{Y_v}(y_v)\mathrm{d}x_u\mathrm{d}y_v \\ &+ \sum_{v=1}^{n}\sum_{u=1}^{m} \iint \mathrm{g}_{j,X_u} \mathrm{g}_{i,Y_v} f_{X_u\left(f_j\right)}(x_u) f_{Y_v}(y_v)\mathrm{d}x_u\mathrm{d}y_v \\ &+ \sum_{v_1=1}^{n}\sum_{v_2=1}^{n} \iint \mathrm{g}_{i,Y_{v_1}} \mathrm{g}_{j,Y_{v_2}} f_{Y_{v_1}}(y_{v_1}) f_{Y_{v_2}}(y_{v_2})\mathrm{d}y_{v_1}\mathrm{d}y_{v_2}.\end{aligned} \tag{24}$$

It can be found that the high dimensional integral in eq. (24) becomes a linear superposition of a plurality of one-dimensional and two-dimensional integrals, wherein every two-dimensional integral function is the product of two univariate functions. When performing numerical integration method to solveeq. (24), we adopt the same integral nodes as which are used for calculating the statistical moments in Sect. 3.2, so that avoid calling the function again, so as to improve the computational efficiency.

Taking solution of eq. (24) into eq. (19), the correlation coefficient of any two discrete frequency points' functions can be calculated. Then the correlation coefficient matrix ρ can be constructed. Finally, the correlation coefficient matrix ρ' corresponding to the standard normal distribution will be obtained by Nataf transformation. Combined with the PDF $f_{g_i}, i = 0, 1, ..., p$, of each discrete frequency point function obtained in Sect. 3.2, the failure probability $P(f_\mathrm{L}, f_\mathrm{U})$ of frequency domain function can be obtained by solving eq. (3). We can also obtain the CDF of the frequency domain function by solving the eq. (3) at different thresholds, and this process does not need additional computational effort. Otherwise, the calculation of the multidimensional Gaussian distribution function in eq. (3) can refer to the refs. [29–33]. It is worth noting that, in the above analysis, all random processes in $X(f)$ are assumed to be mutually independent

and so are all random variables in Y. If they are not independent, the Nataf transformation and the orthogonal transformation can be applied to transform them into mutually independent ones so that the above analysis works as well.

4 Examples and discussion

In this section, three examples are used to demonstrate the accuracy and efficiency of FRDR. As a comparison, MCS are adopted in these examples, in which random process samples are generated by the expansion optimal linear estimation method (EOLE) [34].

4.1 Frequency domain reliability analysis of a numerical example

Construct the frequency domain function as follows:

$$g(x_1,x_2,p(f),f) = 3\mathrm{e}^{-4}x_1x_2f - 1.8\mathrm{e}^{-7}x_2f^2 - 0.5p(f) + 2.01, \tag{25}$$

in which x_1, x_2 are random variables, $P(f)$ is random process, f represents frequency. The distributions of all random parameters are listed in Table 1. It is stipulated that the frequency band is $[f_{\mathrm{L}}, f_{\mathrm{U}}]$, and the allowable minimum is G, then the failure probability of the frequency domain function is given by

$$P(f_{\mathrm{L}},f_{\mathrm{U}},G) = 1 - P\{g(\mathbf{x},p(f),f) \geq G, \forall f \in [f_{\mathrm{L}},f_{\mathrm{U}}]\}, \quad \mathbf{x} = [x_1,x_2,x_3,x_4]. \tag{26}$$

When the threshold $G = 0$, and taking 40 Hz as the center frequency, the frequency domain reliability in different frequency bandwidths is analyzed. Three different Cases 1–3 are considered, where the number of discrete frequency points N is 15, 29 and 43 respectively. The reliability analysis results obtained by FRDR and MCS, and relative error between the two methods are listed in Table 2. In MCS, the number of samples is set to be 1.4×10^9. Figure 2 shows that the failure probability obtained by FRDR and MCS changes with the frequency bandwidth. Firstly, the results indicate that, the reliability does not remain constant but gradually decreases with the increase of frequency bandwidth. Secondly, it shows the stability of FRDR, of which the results gradually approach that of MCS as N increases. In the case of N=43, the minimum correlation coefficient of arbitrary adjacent discrete frequency points' functions is above 0.95, and the curve of this case is very close to that of MCS. In Cases 1–3, the maximum deviations of the failure probability obtained by FRDR are 33%, 10% and 1.5% respectively. That shows a good convergence and accuracy of the method.

From the perspective of computational efficiency, when the frequency band is $[f_{\mathrm{L}},f_{\mathrm{U}}]$=[12,68], MCS called the frequency domain function 1.4×10^9 times, while FRDR called the frequency domain function 360 times, 696 times and 1032 times in Cases 1–3 respectively. So it can be found that FRDR is far more efficient than MCS. In addition, Figure 3 shows the CDF curve of the frequency domain function obtained by MCS and FRDR in Case 3 within the frequency band of $[f_{\mathrm{L}}, f_{\mathrm{U}}]$=[12,68].

4.2 Frequency domain reliability analysis of power amplifier link

The power amplifier link is an important part of the transmit/receive (T/R) module of active phased array radar [35–37]. The frequency domain characteristics of the power amplifier link are the key indicators to measure its performance. And the frequency domain reliability analysis of the power amplifier link can provide an important reference for its design and optimization to improve its performance. The finite element model of the power amplifier link is shown in Figure 4 [38], which is mainly composed of two parts: microstrip lines and printed boards. The printed boards are divided into two types: FR4 printed board and microwave printed board. The material and size parameters are different of them, and so are the microstrip lines' size.

Consider signal transmission process of the power amplifier link. Let the input electromagnetic signal in the power amplifier link be $I_{\mathrm{in}} = A(\cos 2\pi f + \varphi_{\mathrm{in}})$, and the output will be $I_{\mathrm{out}} = nA(\cos 2\pi f + \varphi_{\mathrm{out}})$, where A denotes the amplitude of the input signal, n is the amplification factor, f represents frequency, $\varphi_{\mathrm{in}}, \varphi_{\mathrm{out}}$ represents the input and output phases respectively. In practical application, we are more concerned about the uncertainty of the phase shift $\Delta\varphi = \varphi_{\mathrm{out}} - \varphi_{\mathrm{in}}$, and the phase shift can be expressed as

$$\Delta\varphi = \Delta\varphi(x_1, x_2, x_3, x_4, \varepsilon_1(f), \varepsilon_2(f), f), \tag{27}$$

where x_1,x_3 represent the thickness of FR4 printed board and microwave printed board respectively, x_2, x_4 represent the width of the microstrip line on FR4 printed board and microwave printed board respectively, and they are all regarded as random variables. $\varepsilon_1(f)$, $\varepsilon_2(f)$ represent the permittivity of FR4 printed board and microwave printed board respectively, and they are random processes. The distributions of all random parameters are listed in Table 3. The function involved frequency can be expressed as

$$g(x_1, x_2, x_3, x_4, \varepsilon_1(f), \varepsilon_2(f), f) = \Delta\varphi(x_1, x_2, x_3, x_4, \varepsilon_1(f), \varepsilon_2(f), f) - \mu_{\Delta\varphi}(f). \tag{28}$$

When the frequency band is $[f_{\mathrm{L}},f_{\mathrm{U}}]$, and the allowable minimum phase shift radius is $\Delta\varphi_r$, the failure probability of the power amplifier link is given by

Table 1 Distributions of the random parameters for numerical example

Parameter	Type of distribution	Mean	Coefficient of variation	Autocorrelation coefficient function
x_1	Normal	1.3	0.01	NA
x_2	Normal	1.3	0.05	NA
$p(f)$	Stationary Gaussian process	3	0.3	$\exp[-(0.16\Delta f)^2]$

Table 2 The failure probability of frequency domain function

Result		Frequency (Hz)							
		40	40±4	40±8	40±12	40±16	40±20	40±24	40±28
MC		0.000202	0.000769	0.00136	0.00194	0.00251	0.00308	0.00368	0.00423
FRDR	Case 1	0.000205	0.000581	0.000970	0.00135	0.00172	0.00208	0.00248	0.00290
	relative error	2.0%	24%	29%	30%	32%	33%	33%	30%
	Case 2	0.000205	0.000706	0.00123	0.00179	0.00228	0.00277	0.00330	0.00392
	relative error	1.5%	8.2%	10%	7.7%	9.2%	10%	12%	7.3%
	Case 3	0.000205	0.000763	0.00134	0.00191	0.00252	0.00312	0.00372	0.00428
	relative error	1.5%	0.78%	1.5%	1.5%	0.40%	1.3%	1.1%	1.2%

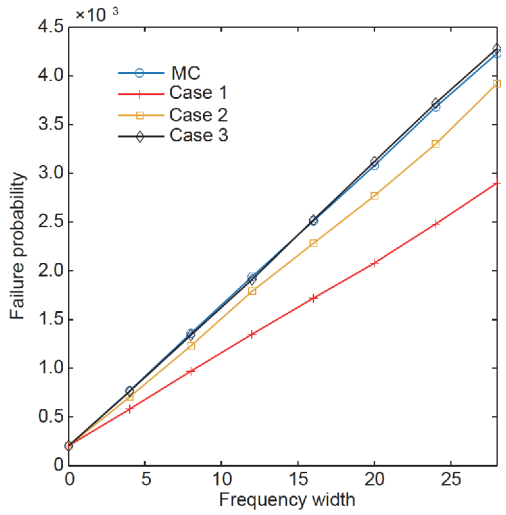

Figure 2 (Color online) The curves indicating the failure probability for the frequency domain function.

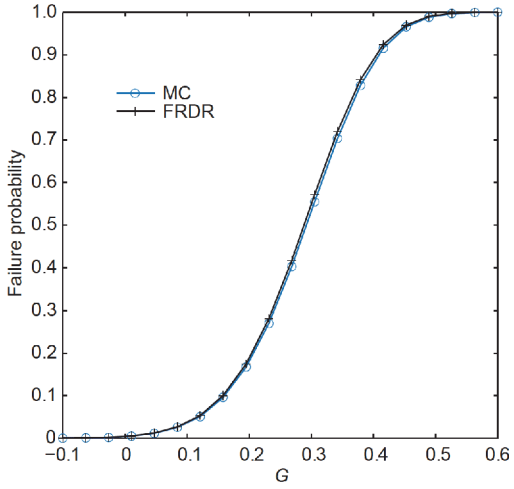

Figure 3 (Color online) The CDF curves of the frequency domain function in the frequency band of $[f_L, f_U]$ = [12, 68].

$$P(f_L, f_U, [\Delta\varphi - \Delta\varphi_r, \Delta\varphi + \Delta\varphi_r]) = 1 - P\left\{\begin{matrix} g(\mathbf{x}, \boldsymbol{\varepsilon}(f), f) > \Delta\varphi - \Delta\varphi_r \\ \cap g(\mathbf{x}, \boldsymbol{\varepsilon}(f), f) < \Delta\varphi + \Delta\varphi_r, \forall f \in [f_L, f_U] \end{matrix}\right\},$$
$$\mathbf{x} = [x_1, x_2, x_3, x_4], \boldsymbol{\varepsilon}(f) = [\varepsilon_1(f), \varepsilon_2(f)]. \quad (29)$$

Perform frequency domain reliability analysis to this problem. In the case of the center frequency is 3 GHz and $\Delta\varphi_r = 5°$, the frequency domain reliability in different frequency bandwidths is analyzed. Three different Cases 1–3 are considered, where the number of discrete frequency points N is 15, 29 and 43, respectively. The reliability analysis results obtained by FRDR and MCS, and relative error between the two methods are listed in Table 4. In MCS, the number of samples is set to be 7×10^6. Figure 5 shows that the failure probability obtained by FRDR and MCS changes with the frequency bandwidth. Firstly, the results indicate that, the reliability does not remain constant but gradually decreases with the increase of frequency bandwidth. Secondly, it shows the stability of FRDR, of which the results gradually approach that of MCS as N increases. In the case of N=43, the minimum correlation coefficient of arbitrary adjacent discrete frequency points' functions is above 0.96, and the curve of this case is very close to that of MCS. In Cases 1–3, the maximum deviations of the failure probability obtained by FRDR are 4.3%, 2.3% and 1.2%, respectively. That shows a good convergence and accuracy of the method. From the perspective of computational efficiency, when the frequency band is $[f_L, f_U]$=[2.3,3.7], MCS called the frequency domain function 7×10^6 times, while FRDR called the

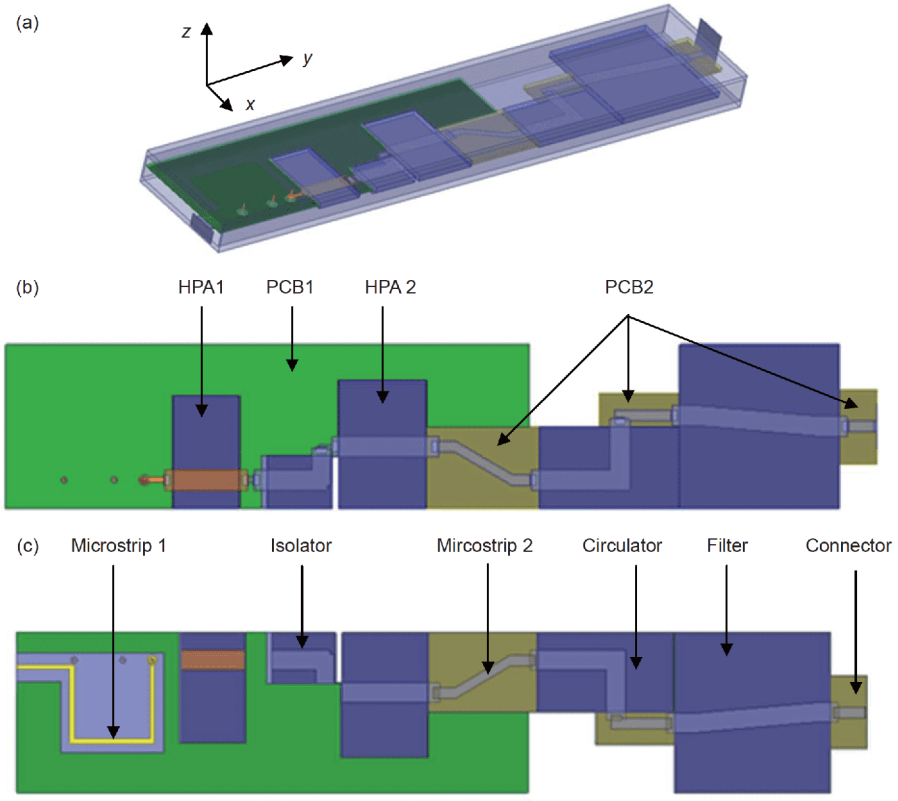

Figure 4 (Color online) Finite element model of the power amplifier link [38]. (a) 3D electromagnetic simulation model; (b) top view of the model without the shell; (c) bottom view of the model without the shell.

Table 3 Distributions of the random parameters for the power amplifier link

Parameter	Type of distribution	Mean	Coefficient of variation	Autocorrelation coefficient function
x_1	Lognormal	0.7 mm	0.0014	NA
x_2	Lognormal	0.9 mm	0.0019	NA
x_3	Normal	1 mm	0.001	NA
x_4	Normal	2.2 mm	0.0015	NA
$\varepsilon_1(f)$	Stationary Gaussian process	4.8	0.069	$\exp[-(0.9f)^2]$
$\varepsilon_2(f)$	Stationary Gaussian process	3.5	0.049	$\exp[-(0.9f)^2]$

Table 4 The failure probability of the power amplifier link

Result		Frequency (Hz)							
		3	3±0.1	3±0.2	3±0.3	3±0.4	3±0.5	3±0.6	3±0.7
MC		0.0263	0.0322	0.0332	0.0349	0.0372	0.0386	0.0395	0.0404
FRDR	Case 1	0.0265	0.0304	0.0318	0.0334	0.0358	0.0374	0.0385	0.0397
	relative error	0.76%	2.25%	4.22%	4.30%	3.76%	3.11%	2.53%	1.73%
	Case 2	0.0265	0.0308	0.0325	0.0341	0.0366	0.0382	0.0390	0.0399
	relative error	0.76%	0.96%	2.11%	2.29%	1.61%	1.04%	1.27%	1.24%
	Case 3	0.0265	0.0309	0.0328	0.0345	0.0369	0.0383	0.0393	0.0400
	relative error	0.76%	0.64%	1.20%	1.15%	0.81%	0.78%	0.51%	0.99%

frequency domain function 450 times, 870 times and 1290 times in Cases 1–3 respectively. So it can be found that FRDR is far more efficient than MCS. In addition, we can see that the power amplifier link has a good reliability at the center frequency, and its failure probability is 0.0265. However, when the frequency bandwidth is up to 1.4 GHz,

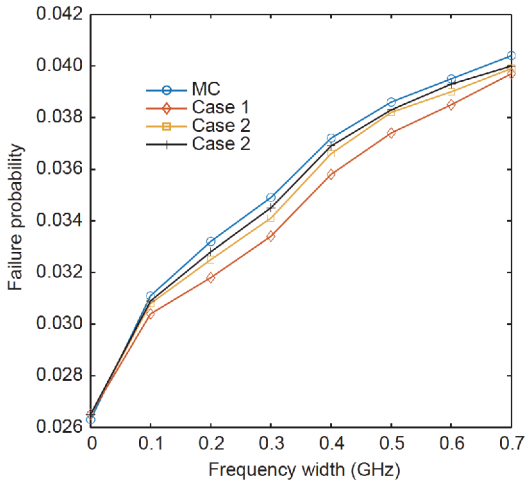

Figure 5 (Color online) The curves indicating the failure probability for the power amplifier link.

the failure probability increases to 0.0400, about 1.5 times the initial value. So its reliability in supposed bandwidth should be taken into account when the power amplifier link is in the part of design. When the frequency bandwidth is 1.4 GHz, Figure 6 shows that the failure probability of the power amplifier link varies with phase shift radius within the frequency band of $[f_{\mathrm{L}}, f_{\mathrm{U}}] = [2.3, 3.7]$.

4.3 Frequency domain reliability analysis of phased-array antenna

Phased-array antenna has been widely used and rapidly developed in the fields of radar, communication, electronic warfare, and navigation [8–10]. Its frequency domain performances are the main objectives in design and optimization. The reliability analysis of frequency domain performances can provide an important reference for design and optimization under uncertainty, and further improve the performances. Figure 7 shows the finite element model of a horn phased array antenna, which is consisted of four identical horn antennas. Each horn antenna has an independent input current. Focus on the electric field intensity in frequency domain, and it can be influenced by the phase errors of the input currents and the structural errors of the antenna. The structural errors are mainly from the heights of the waveguides z_1, z_2, z_3, z_4 and the horns z_5, z_6, z_7, z_8, that are all regarded as random variables. The input currents' phases are related to frequency, and are expressed as $\alpha_1(f), \alpha_2(f), \alpha_3(f), \alpha_4(f)$, that are regarded as random processes. The distributions of the random parameters described above are shown in Table 5. Considering the these variables, the electric field intensity of the array antenna can be expressed as

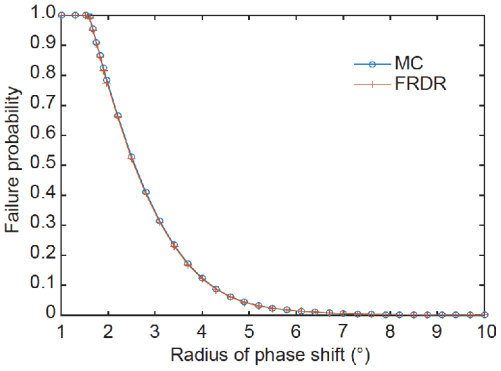

Figure 6 (Color online) The failure probability of the power amplifier link varies with phase shift radius.

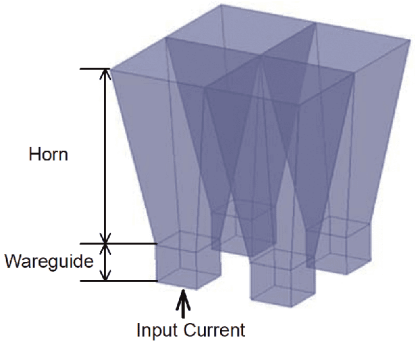

Figure 7 (Color online) Finite element model of the horn phased array antenna.

$$\begin{aligned}\mathbf{E}(\theta,\varphi) &= \mathbf{E}_1+\mathbf{E}_2+\mathbf{E}_3+\mathbf{E}_4\\ &= \mathbf{B}(\theta,\varphi)\left[A_1\mathrm{e}^{j\alpha_1(f)}+A_2\mathrm{e}^{j\alpha_2(f)}\right.\\ &\quad \left.+A_3\mathrm{e}^{j\alpha_3(f)}+A_4\mathrm{e}^{j\alpha_4(f)}\right],\end{aligned} \tag{30}$$

where $B(\theta,\varphi)$ is related to antenna structure which can be seen as the function of z_1–z_8, θ,φ represents the direction angle of the spherical coordinate system, $A_i, i = 1,2,3,4$ is the current amplitude. In the case of $\theta = 0, \varphi = 0$, the frequency domain function $E(0,0)$ can be expressed as

$$\begin{aligned}&\mathrm{g}\left(z_1,z_2,\ldots,z_8,\alpha_1(f),\alpha_2(f),\alpha_3(f),\alpha_4(f)\right)\\ &= \mathbf{B}(0,0)\left[A_1\mathrm{e}^{j\alpha_1(f)}+A_2\mathrm{e}^{j\alpha_2(f)}+A_3\mathrm{e}^{j\alpha_3(f)}+A_4\mathrm{e}^{j\alpha_4(f)}\right].\end{aligned} \tag{31}$$

When the frequency band is $[f_{\mathrm{L}}, f_{\mathrm{U}}]$, and the allowable minimum electric field intensity is G, the failure probability of the phased array antenna is given by

$$\begin{aligned}&P(f_{\mathrm{L}},f_{\mathrm{U}},G) = 1-P\{g(\mathbf{z},\boldsymbol{\alpha}(f))\geq G,\forall f\in[f_{\mathrm{L}},f_{\mathrm{U}}]\},\\ &\mathbf{z} = [z_1,z_2,\ldots,z_8],\ \boldsymbol{\alpha}(f) = [\alpha_1(f),\alpha_2(f),\alpha_3(f),\alpha_4(f)].\end{aligned} \tag{32}$$

Perform frequency domain reliability analysis to this problem. In the case of G=43.8 dB and the center frequency is 9 GHz, the frequency domain reliability in different frequency bandwidths is analyzed. Three different Cases 1–3

Table 5 Distributions of the random parameters for the horn phased array antenna

Parameter	Type of distribution	Mean	Sigma	Autocorrelation coefficient function
z_1–z_4	Normal	29 mm	0.29 mm	NA
z_5–z_8	Lognormal	165 mm	0.297 mm	NA
$\alpha_1(f)$–$\alpha_4(f)$	Stationary Gaussian process	0°	15°	$\exp[-(0.75\,f)^2]$

Table 6 The failure probability of the phased-array antenna

	Result	Frequency (Hz)										
		9	9±0.05	9±0.1	9±0.15	9±0.2	9±0.25	9±0.3	9±0.35	9±0.4	9±0.45	9±0.5
FRDR	MC	0.0136	0.0259	0.0396	0.0528	0.0611	0.0635	0.0651	0.0677	0.0705	0.0801	0.0898
	Case 1	0.0139	0.0239	0.0356	0.0468	0.0518	0.0537	0.0553	0.0571	0.0603	0.0691	0.0793
	relative error	2.21%	7.72%	10.10%	11.36%	15.22%	15.43%	15.05%	15.66%	14.47%	13.73%	11.69%
	Case 2	0.0139	0.0249	0.0380	0.0512	0.0591	0.0609	0.0622	0.0639	0.0671	0.0758	0.0855
	relative error	2.21%	3.86%	4.04%	3.03%	3.27%	4.09%	4.45%	5.61%	4.82%	5.37%	4.79%
	Case 3	0.0139	0.0256	0.0391	0.0521	0.0602	0.0623	0.0643	0.0660	0.0695	0.0783	0.0887
	relative error	2.21%	1.16%	1.26%	1.33%	1.47%	1.89%	1.23%	2.51%	1.42%	2.25%	1.22%

are considered, where the number of discrete frequency points N is 21, 41 and 61 respectively. The reliability analysis results obtained by FRDR and MCS, and relative error between the two methods are listed in Table 6. In MCS, the number of samples is set to be 1×10^7. Figure 8 shows that the failure probability obtained by FRDR and MCS changes with the frequency bandwidth. Firstly, the results indicate that, the reliability does not remain constant but gradually decreases with the increase of frequency bandwidth. Secondly, it shows the stability of FRDR, of which the results gradually approach that of MCS as N increases. In the case of N=61, the minimum correlation coefficient of arbitrary adjacent discrete frequency points' functions is above 0.95, and the curve of this case is very close to that of MCS. In Cases 1–3, the maximum deviations of the failure probability obtained by FRDR are 15%, 5.6% and 2.5%, respectively. That shows a good convergence and accuracy of the method. From the perspective of computational efficiency, when the frequency band is [f_L, f_U]=[8.5,9.5], MCS called the frequency domain function 1×10^7 times, while FRDR called the frequency domain function 1260 times, 2460 times and 3660 times in Cases 1–3 respectively. So it can be found that FRDR is far more efficient than MCS. In addition, we can see that the power amplifier link has a good reliability at the center frequency, and its failure probability is 0.0139. However, when the frequency bandwidth is up to 1 GHz, the failure probability increases to 0.0887, about 6 times the initial value. So its reliability in supposed bandwidth should be taken into account when the power amplifier link is in the part of design. When the frequency bandwidth is 1 GHz, Figure 9 shows that the failure probability of the array antenna varies with electric field intensity within the frequency

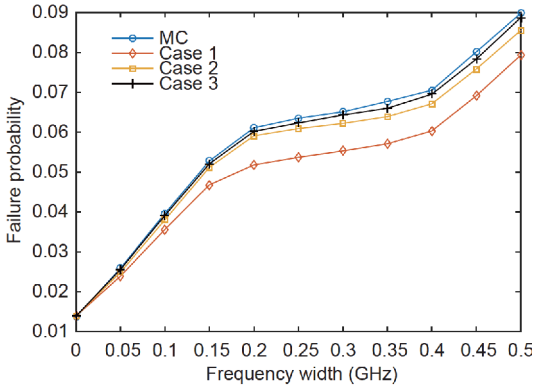

Figure 8 (Color online) The curves indicating the failure probability for the phased array antenna.

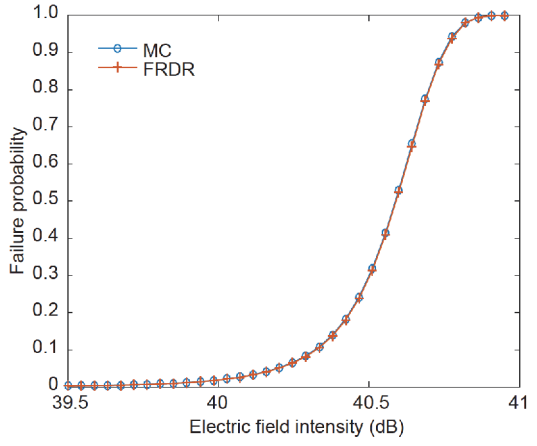

Figure 9 (Color online) The failure probability of the phased array antenna varies with electric field intensity.

band of $[f_L, f_U]$=[8.5,9.5].

5 Conclusions

In electromagnetic problems, the reliability in frequency band is usually lower than the reliability of center frequency, and the wider the bandwidth, the greater the probability of failure. This paper defines the frequency domain reliability problem of electromagnetic problems, and proposes a frequency domain reliability method based on UDRM, which provides an effective calculation tool for practical electromagnetic frequency domain problems. The method firstly discretizes the frequency domain function into a series of frequency points' functions, and then transforms the frequency domain reliability problem into a series system reliability problem of discrete frequency points' functions. And UDRM is introduced to solve the PDFs and correlation coefficients of discrete frequency points' functions, leading to a much higher efficiency. In the future, FRDR can be extended to frequency domain system reliability analysis, frequency domain reliability-based design optimization (FRBDO), and other relevant important issues.

This work was supported by the National Natural Science Foundation of China (Grant No. 51490662), and the National Science Fund for Distinguished Young Scholars (Grant No. 51725502).

1 Jung J. A compact broadband antenna with an L-shaped notch. IEICE Trans Commun, 2006, E89-B: 1968–1971
2 Abbas-Azimi M, Mazlumi F, Behnia F. Design of broadband constant-beamwidth conical corrugated-horn antennas [Antenna Designer's Notebook]. IEEE Antennas Propag Magazine, 2010, 51: 109–114
3 Yang F, Zhou L, Han W, et al. Bandwidth enhancement for single-feed circularly polarised microstrip antenna with epsilon-negative transmission line-based annular ring. Electron Lett, 2015, 51: 1475–1476
4 Klymyshyn D M, Shafai L, Rashidian A. Tall microstrip transmission lines for dielectric resonator antenna applications. IET Microw Antennas Propag, 2014, 8: 112–124
5 Choo H, Ling H. Design of broadband and dual-band microstrip antennas on a high-dielectric substrate using a genetic algorithm. IEE Proc Microw Antennas Propag, 2003, 150: 137–142
6 Mohamadi Monavar F, Komjani N, Mousavi P. Application of invasive weed optimization to design a broadband patch antenna with symmetric radiation pattern. Antennas Wirel Propag Lett, 2011, 10: 1369–1372
7 Abbas-Azimi M, Arazm F, Faraji-Dana R. Design and optimisation of a high-frequency EMC wideband horn antenna. IET Microw Antennas Propag, 2007, 1: 580
8 Pourahmadazar J, Rafii V. Broadband circularly polarised slot antenna array for L- and S-band applications. Electron Lett, 2012, 48: 542–543
9 El-makadema A, Rashid L, Brown A K. Geometry design optimization of large-scale broadband antenna array systems. IEEE Trans Antennas Propagat, 2014, 62: 1673–1680
10 Wang P, Li Y, Peng Y, et al. Non-uniform linear antenna array design and optimization for millimeter-wave communications. IEEE Trans Wireless Commun, 2016, 15: 7343–7356
11 Okabe H, Caloz C, Itoh T. A compact enhanced-bandwidth hybrid ring using an artificial lumped-element left-handed transmission-line section. IEEE Trans Microwave Theor Techn, 2004, 52: 798–804
12 Kim D, Kim H, Eo Y. A novel transmission line characterisation based on measurement data reconfirmation. Int J Electron, 2014, 101: 479–491
13 You F, Hu Z, Ding X, et al. 2–4 GHz wideband power amplifier with ultra-flat gain and high PAE. Electron Lett, 2013, 49: 326
14 Jiang C, Huang X P, Han X, et al. A time-variant reliability analysis method based on stochastic process discretization. J Mech Des, 2014, 136: 091009
15 Rackwitz R, Flessler B. Structural reliability under combined random load sequences. Comput Struct, 1978, 9: 489–494
16 Hasofer A M. Exact and invariant second-moment code format. J Eng Mech Division, 1974, 100: 111–121
17 Hohenbichler M, Rackwitz R. Zon-normal dependent vectors in structural safety. J Eng Mech Division, 1981, 107: 1227–1238
18 Breitung K. Asymptotic approximations for multinormal integrals. J Eng Mech, 1984, 110: 357–366
19 Cai G Q, Elishakoff I. Refined second-order reliability analysis. Struct Saf, 1994, 14: 267–276
20 Rahman S, Xu H. A univariate dimension-reduction method for multi-dimensional integration in stochastic mechanics. Probab Eng Mech, 2004, 19: 393–408
21 Xu H, Rahman S. A generalized dimension-reduction method for multi-dimensional integration in random mechanics. Int J Numer Methods Eng, 2006, 65: 2292
22 Huang B, Du X. Uncertainty analysis by dimension reduction integration and saddlepoint approximations. J Mech Des, 2006, 128: 26
23 Andrieu-Renaud C, Sudret B, Lemaire M. The PHI2 method: A way to compute time-variant reliability. Reliability Eng Syst Saf, 2004, 84: 75–86
24 Jaynes E T. Information theory and statistical mechanics. Phys Rev, 1957, 106: 620–630
25 Hohenbichler M, Rackwitz R. First-order concepts in system reliability. Struct Saf, 1982, 1: 177–188
26 Siddall J N, Diab Y. The use in probabilistic design of probability curves generated by maximizing the shannon entropy function constrained by moments. J Eng Industry, 1975, 97: 843
27 Stump D, Pumplin J, Brock R, et al. Uncertainties of predictions from parton distribution functions i: the lagrange multiplier method. Phys Rev D Part Fields, 2001, 65: 360–363
28 Durante F, Sempi C. Copula Theory: An Introduction. In: Copula Theory and Its Applications. Berlin, Heidelberg: Springer, 2010. 3–31
29 Nadarajah S. On the approximations for multinormal integration. Comput Indust Eng, 2008, 54: 705–708
30 Pandey M D. An effective approximation to evaluate multinormal integrals. Struct Saf, 1998, 20: 51–67
31 Genz A, Bretz F. Computation of multivariate normal and *t* probabilities. J Statist Software, 2010, 33: 1641
32 Genz A. Numerical computation of multivariate normal probabilities. J Comput Graph Stat, 1992, 1: 141–149
33 Tang L K, Melchers R E. Improved approximation for multinormal integral. Struct Saf, 1986, 4: 81–93
34 Li C, Der Kiureghian A. Optimal discretization of random fields. J Eng Mech, 1993, 119: 1136–1154
35 Yeo S K, Chun J H, Kwon Y S. A 3-D X-band T/R module package with an anodized aluminum multilayer substrate for phased array radar applications. IEEE Trans Adv Packag, 2011, 33: 883–891
36 Porras M J P, Bertuch T, Loecker C, et al. An AESA antenna comprising an RF feeding network with strongly coupled antenna ports. IEEE Trans Antennas Propag, 2015, 63: 182–194
37 Ahn C S, Chon S M, Kim S J, et al. Accurate characterization of T/R modules with consideration of amplitude/phase cross effect in AESA antenna unit. ETRI J, 2016, 38: 417–424
38 Wang Z H, Jiang C, Ruan X X, et al. Uncertainty propagation analysis of T/R modules. Int J Comput Methods, 2018, 38: 1850105